Tomasz NOWAK[1], Krzysztof DUDEK[1], Piotr PIEKARSKI[2]

ABB Corporate Research, Krakow (1), ABB Power Products Medium Voltage, Przasnysz (2)

Fast algorithm for numerical analysis of electro-mechanical behaviour of busbar systems

***Abstract**. The article is focused on numerical analysis of electro-mechanical forces in busbar systems, used especially in MV applications. The theoretical background for fast derivation of magnetic induction values, respective Lorentz forces, as well as mechanical response (deformations, and stresses) has been presented. The paper provides implementation remarks, describes verification examples, and compares them with real measurement data.*

***Streszczenie.** W artykule przedstawiono sposób numerycznej analizy przewodów prądowych, stosowanych zwłaszcza w szynoprzewodach instalacji SN. Podano teoretyczne podstawy wyznaczania indukcji magnetycznej oraz sił Lorentza występujących w przewodnikach prądowych w stanie zwarcia, oraz podano metodykę określania odkształceń i naprężeń mechanicznych. Przedstawiono informacje na temat praktycznej implementacji zaproponowanego algorytmu, a także podano przykłady obliczeniowe i eksperymentalne, które pozytywnie weryfikowały zaprezentowaną metodę analizy. (**Szybki algorytm analizy numerycznej wspomagający obliczenia elektro-mechaniczne szynoprzewodów**).*

Keywords: Lorentz forces, mechanical displacements and stresses, busbar systems.
Słowa kluczowe: siły Lorentza, przemieszczenia i naprężenia, szynoprzewody.

Introduction

Three-phase busbar systems are commonly used in power distribution network as vital components of substations or MV switchgears. To achieve a reliable mechanical behaviour of phase buses, their design must consider magnetic, thermal and material aspects, with respect to the most severe loads. Since very high current strengths, that may occur during a short-circuit event, can drive to permanent deformation of the current conductor, the proper determination of maximal electro-mechanical forces is an important design problem. The investigation of conductor withstand is not a new engineering topic, therefore over last decades several analysis methods have been proposed. Some of them utilize simplified analytical theories [1,2], while others involve also experimental or semi-empirical factors (e.g. Dwight's charts) [3]. There are also calculation approaches recommended by international standards or committees [4,5,6], and some of the market players [7,8].

With increasing popularity of modern numerical methods [9-12], high reliability of results was achieved, and even very complex electro-mechanical problems can be solved today. The commercially available software packages, like ANSYS or ABAQUS, allow studying various types of electric, magnetic, thermal and mechanical aspects, coupling them together. However, for some special applications, the general-purpose Finite Element Method (FEM) packages may seem cumbersome, and the same results can be accomplished much faster with use of specialized tools. It relates especially to the electro-mechanical analysis of busbar structures, which can be geometrically simplified to line elements (since length of the conductor is much larger than two other dimensions of its cross-section). Such a simple numerical case can be efficiently solved by dedicated one-dimensional element, which is not offered by commercial FEM packages (for electro-dynamic analysis they offer more complex 2D and 3D elements only, [13,14]).

This paper introduces the concept of a FEM beam element, which reacts to electro-mechanical loads driven by the magnetic field. First, the theoretical background of the problem is shortly stated. In following paragraph, the detailed description of the calculation procedure is provided, while next section contains an exemplary numerical case, which was compared with real-life test results. The conclusions and final remarks are given in last chapter.

Theoretical Basis

The literature provides two main methods for calculating electro-dynamic forces within the current conductors. The first approach derives the magnetic field created by an electrical current at a point in space. Based on that value, it calculates the force acting at this point of a conductor through which an electrical current flows (possibly these two currents are different). In order to determine the magnetic field, the Biot-Savart law is most commonly used (or Ampere's theorem, which is deducted from it). This relation states, that each element (i), Figure 1, of a circuit energized by a current (I_i), of an infinite small length ($\mathrm{d}\boldsymbol{l}_i$) produces at a point j a magnetic field $\mathrm{d}\boldsymbol{B}_{ji}$ such that:

(1) $$\mathrm{d}\overrightarrow{B_{ji}} = \frac{\mu_0}{4\pi} I_i \frac{\mathrm{d}\overrightarrow{l_i} \times \overrightarrow{r_{ij}}}{r_{ij}^3}$$

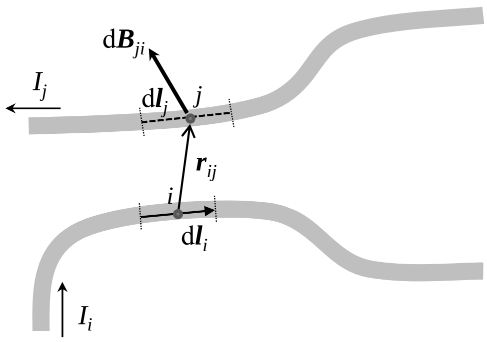

Fig.1. Graphical explanation of Biot-Savart law

To calculate the electro-dynamic force, the Laplace's formula is applied (2). It states, that each infinite small element ($\mathrm{d}\boldsymbol{l}_j$) of a circuit energized by a current (I_j), which is placed in a magnetic field ($\boldsymbol{B}$), is subjected to a force ($\mathrm{d}\boldsymbol{f}_j$) equals to:

(2) $$\mathrm{d}\overrightarrow{f_j} = I_j \cdot \mathrm{d}\overrightarrow{l_j} \times \overrightarrow{B}$$

Elements i and j may either belong to different electrical circuits (phases), or can be the part of the same current conductor (in this case $I_i = I_j$).

The second analysis method uses Maxwell's theorem and is based on calculating the potential energy variation of a circuit. The mechanical force acting on a circuit is related to the change of magnetic flux and the current flowing through the conductor:

(3) $$F_x = i\frac{\delta\Phi}{\delta x}$$

and likewise for F_y and F_z in their respective directions.

The results obtained by first or second approach may differ slightly, since underlying assumptions for these theorems were not the same. In this paper, authors apply the calculation method based on (1) and (2), and expended it further about geometrical and stiffness relations in order to derive mechanical response of the structure under study.

Numerical Implementation

The concept of numerical electro-mechanical analysis of the busbar structure can be described by following procedure:

- The geometry of the busbars is defined by a set of line segments oriented freely in 3D space; The conductor is reduced to a center line only, while the cross-section is thus represented by a point having its geometrical properties (like cross-section area and area moments of inertia);
- Each line segment is divided into finite elements, which are joined in nodes; Each finite element consists of 2 nodes, Figure 2;
- Each node has 6 mechanical degrees of freedom (DOF) - 3 translations, U, and 3 rotations, R;
- Magnetic induction vector, $\boldsymbol{B}$ is calculated in the center of each finite element, based on the electrical current flowing through all other elements;
- Lorentz force is derived in the center of each finite element, based on the electrical current flowing through this element and its magnetic induction;
- Lorentz force is distributed into nodes, as mechanical Load vector, $\{F\}$;
- Global Stiffness matrix, $[K]$, describing the mechanical stiffness of the whole busbar structure, is aggregated out of the local stiffness matrixes of all finite elements;
- Nodal Displacement vector $\{U\}$ (deformation of the busbar structure) is derived based on Load vector and Global Stiffness matrix;
- Mechanical stress in every finite element is calculated, based on nodal displacements and element stiffness properties.

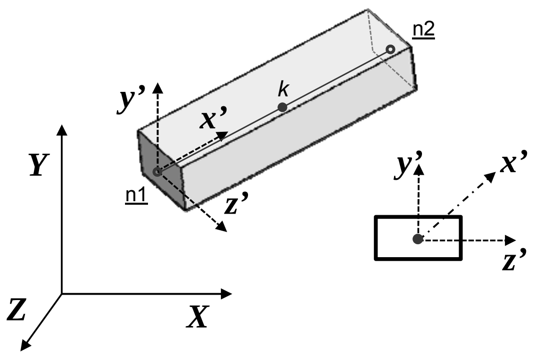

Fig.2. Coordinate systems: global (XYZ) and local (x'y'z') used for k-th element having two nodes (n1, n2)

Numerically, the vector of magnetic induction, B_i at the center of i-th element may be described as the sum over all M-segments of the complete busbar system:

(4) $$B_i = \begin{bmatrix} B_{iX} \\ B_{iY} \\ B_{iZ} \end{bmatrix} = \frac{\mu_0}{4\pi}\sum_{j=1}^{M}\frac{I_j}{r_{ij}^{3}}\begin{vmatrix} 1 & 1 & 1 \\ \mathrm{d}l_{jX} & \mathrm{d}l_{jY} & \mathrm{d}l_{jZ} \\ r_{ijX} & r_{ijY} & r_{ijZ} \end{vmatrix}$$

where: $\mathrm{d}l_{jk}$ – length of the j-th element in respective k-direction [m], r_{ij} – distance between centers of i-th and j-th elements with respective directional components [m], I_j – electrical current in j-th element [A].

Based on (2) the incremental Lorentz force acting on i-th element can be calculated as:

(5) $$\mathrm{d}F_i = \begin{bmatrix} \mathrm{d}F_{iX} \\ \mathrm{d}F_{iY} \\ \mathrm{d}F_{iZ} \end{bmatrix} = I_i\begin{vmatrix} 1 & 1 & 1 \\ \mathrm{d}l_{iX} & \mathrm{d}l_{iY} & \mathrm{d}l_{iZ} \\ B_{iX} & B_{iY} & B_{iZ} \end{vmatrix}$$

where: dl_{ik} – length of the i-th element in respective k-direction [m], B_{ik} – k-direction component of magnetic induction [T], I_i – electrical current in i-th element [A].

Please note, that $\mathrm{d}F_i$, (5), was calculated for the center of i-th element. For further mechanical calculations it is required to distribute this lamped load into forces and moments at two FE nodes belonging to this element. When introducing directional components of forces and moments for 1st and 2nd node respectively, the load vector for a single finite element will have the following form:

(6) $$\{F_i^{\,e}\} = \begin{bmatrix} \begin{vmatrix} \frac{\mathrm{d}F_{iX}}{2} & \frac{\mathrm{d}F_{iY}}{2} & \frac{\mathrm{d}F_{iZ}}{2} & 0 & -\frac{\mathrm{d}F_{iZ}\mathrm{d}l_i}{12} & \frac{\mathrm{d}F_{iY}\mathrm{d}l_i}{12} \end{vmatrix}^T \\ \begin{vmatrix} \frac{\mathrm{d}F_{iX}}{2} & \frac{\mathrm{d}F_{iY}}{2} & \frac{\mathrm{d}F_{iZ}}{2} & 0 & \frac{\mathrm{d}F_{iZ}dl}{12} & -\frac{\mathrm{d}F_{iY}\mathrm{d}l_i}{12} \end{vmatrix}^T \end{bmatrix}$$

The global load vector $\{F\}$, describing six Lorentz load components for all N-nodes, can be formed by summing individual forces and moments for the nodes, which are shared between neighbouring elements.

In static analysis the mechanical response of the structure under consideration is calculated based on fundamental equation:

(7) $$\{F\} = [K]\{U\}$$

where: K – is a global stiffness matrix (described by structure stiffness), and U – is a global displacement vector (unknown, to be found).

Since the global load vector $\{F\}$ is derived based on (6), the global stiffness matrix $[K]$ of the whole busbar structure must be provided. It is assembled by elemental stiffness matrixes $[K^e]$, defined for each beam element as below:

(8) $$[K^e] = [T]^T[k^e][T]$$

where: $[k^e]$ – stiffness matrix for a single finite element, in local co-ordinate system; and $[T]$ – is the transformation matrix (from local to global co-ordinate system).

Both matrixes have a quite complex form. The first one represents stiffness of a single element being subjected to axial, bending and torsional forces and corresponding moments:

(9)

$$
\left[k^{e}\right]=\begin{bmatrix}
\frac{EA}{L} & 0 & 0 & 0 & 0 & 0 & -\frac{EA}{L} & 0 & 0 & 0 & 0 & 0 \\
 & \frac{12EI_Z}{L^3} & 0 & 0 & 0 & \frac{6EI_Z}{L^2} & 0 & -\frac{12EI_Z}{L^3} & 0 & 0 & 0 & \frac{6EI_Z}{L^2} \\
 & & \frac{12EI_Y}{L^3} & 0 & -\frac{6EI_Y}{L^2} & 0 & 0 & 0 & -\frac{12EI_Y}{L^3} & 0 & -\frac{6EI_Y}{L^2} & 0 \\
S & & & \frac{GJ}{L} & 0 & 0 & 0 & 0 & 0 & -\frac{GJ}{L} & 0 & 0 \\
 & Y & & & \frac{4EI_Y}{L} & 0 & 0 & 0 & \frac{6EI_Y}{L^2} & 0 & \frac{2EI_Y}{L} & 0 \\
 & & M & & & \frac{4EI_Z}{L} & 0 & -\frac{6EI_Z}{L^2} & 0 & 0 & 0 & \frac{2EI_Z}{L} \\
 & & & M & & & \frac{EA}{L} & 0 & 0 & 0 & 0 & 0 \\
 & & & & E & & & \frac{12EI_Z}{L^3} & 0 & 0 & 0 & -\frac{6EI_Z}{L^2} \\
 & & & & & T & & & \frac{12EI_Y}{L^3} & 0 & \frac{6EI_Y}{L^2} & 0 \\
 & & & & & & R & & & \frac{GJ}{L} & 0 & 0 \\
 & & & & & & & I & & & \frac{4EI_Y}{L} & 0 \\
 & & & & & & & & C & & & \frac{4EI_Z}{L}
\end{bmatrix}
$$

where: A, I_Z, I_y, J – cross-section properties (cross-section area, area moments of inertia, and St Venant torsional stiffness, respectively); E, G – material properties (Young modulus, and Kirchhoff modulus, respectively); and L – element length.

The transformation matrix [*T*] is defined for each element by four directional cosines matrixes [*G*]:

(10)
$$
\left[T\right]=\begin{bmatrix} [G] & 0 & 0 & 0 \\ & [G] & 0 & 0 \\ & & [G] & 0 \\ symm. & & & [G] \end{bmatrix}
$$

The directional cosines matrix represents spatial orientation of the element, and can be calculated as:

(11)
$$
\left[G\right]=\begin{bmatrix} 1 & 0 & 0 \\ 0 & \cos\alpha & \sin\alpha \\ 0 & -\sin\alpha & \cos\alpha \end{bmatrix}\begin{bmatrix} L_X/L & L_Y/L & L_Z/L \\ L_Y/DL & L_X/DL & 0 \\ -L_X L_Z/DL^2 & -L_Y L_Z/DL^2 & D \end{bmatrix}
$$

where: L_K – respective directional components of element length; D = sqrt(L_X^2 + L_Y^2) / L, and α - an angle of the element rotation about its longitudinal axis.

Since the geometry is the busbar element is simplified to the line, the rotation angle α is used to specify how the conductor's cross-section is oriented about its axial direction, Figure 3. It is especially important for mechanical results, because the calculated deflection depends on the conductor's stiffness (which is affected by orientation of the cross-section).

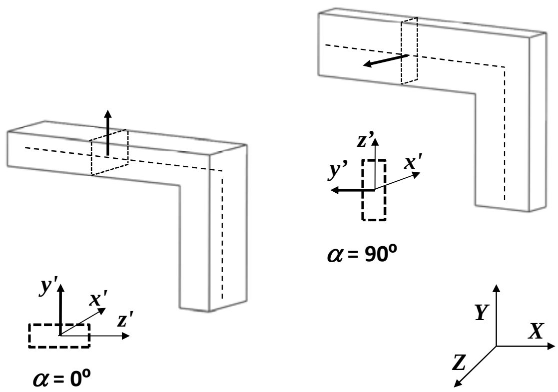

Fig.3. Different orientation of the element (α = 0°, α = 90°)

After introduction of boundary conditions (mechanical fixations), which just zeroes respective columns in global stiffness matrix [*K*], the equation 8 is solved for {*U*}. At the end of the solving procedure vector {*U*} contains displacements (U_X, U_Y, U_Z) and rotations (R_X, R_Y, R_Z) for all nodes within analyzed structure:

(12)
$$
\{U\}=\left[U_{X1} \quad U_{Y1} \quad U_{Z1} \quad R_{X1} \quad R_{Y1} \quad R_{Z1} \quad U_{X2} \quad \ldots \quad R_{ZN}\right]^T
$$

At the final stage, the generalized displacements should be transferred into local co-ordinate systems of individual elements using the transformation matrix [*T*], and mechanical stresses in the center of each element may be derived as:

(13)
$$
\begin{bmatrix} \sigma_{Axial} \\ \sigma_{BendYY} \\ \sigma_{BendZZ} \\ \sigma_{Torsion} \end{bmatrix}=\begin{bmatrix} \frac{E}{L}\left(U_{X2}-U_{X1}\right) \\ \frac{EI_Z}{LW_Z}\left(R_{Z2}-R_{Z1}\right) \\ \frac{EI_Y}{LW_Y}\left(R_{Y2}-R_{Y1}\right) \\ \frac{GJ_O}{LW_O}\left(R_{X2}-R_{X1}\right) \end{bmatrix}
$$

where indexes "1" and "2" refer to first and second nodes of the element, respectively.
Because, both: axial and bending stress components cause the same effect (tension or compression of external layers of the beam) – thus their values should be superimposed. For "rectangular" cross-section, the most severe stress in longitudinal direction can be calculated as:

(14)
$$
\sigma_{MAX}=\sigma_{BendYY}+\sigma_{BendZZ}+\sigma_{Axial}
$$

and this value relates to the corner of the cross-section.

The calculation procedure presented above allows to find out all electromagnetic, as well as mechanical unknowns of the examined busbar structure, namely: magnetic induction values, Lorentz force loads, mechanical deformations and related mechanical stresses.
Moreover, since the presented procedure may be introduced using an iteration approach, the nonlinear relations, which are driven, for example, by temperature dependence on material properties, can be also covered.

The practical implementation of equations 4-14 into numerical code is not a complex task, and it can be managed using even an ordinary spreadsheet program, such as MS/Excel. The demonstration version of the spreadsheet implementation is available from the corresponding author upon request.

Validation Cases

The validation of the proposed calculation method was managed in two ways. First, geometrically simple scenarios, having known theoretical solutions, were compared with the results provided by the developed piece of software. Several combinations of parallel, perpendicular and non-rectilinear 2 and 3-phase systems were checked, showing a very good agreement. For example, the theoretical solution for two parallel conductors of unequal length, Figure 4, specifies the mutual electro-dynamic force as:

(15)
$$
F_Y=\pm\frac{\mu_0}{4\pi}\frac{i_1 i_2}{y}\left(AD-AC+BC-BD\right)
$$

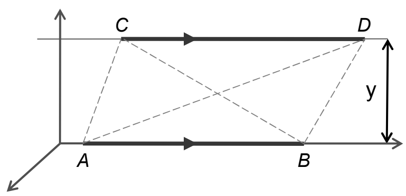

Fig.4. EM force acting between two parallel, but unequal conductors

The analytical solution for a specified geometry (i_1=i_2=1000A, x_A=1, x_B=10, x_C=2, x_B=12, and y=1m) gives F=±1.545N, while the numerical procedure resulted in F=±1.546N, which is below 0.1% of difference.

The theoretical solutions provide exact results for simple cases, but they are not able however to describe more complex geometries. It relates especially to the situation, where two conductors are spaced very close to each other, and their mechanical deformation affected by Lorentz force, strongly influences the source of their deformation. This is highly non-linear case, which can be either verified by real measurements, or calculated numerical by an incremental procedure. Figure 5 presents an example of such a circuit.

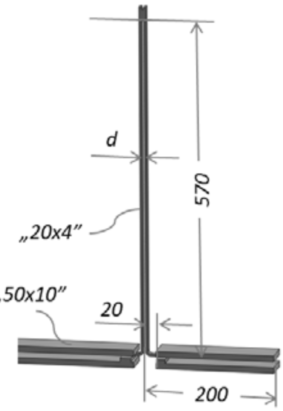

Fig.5. The test circuit used for measurements, which validated the proposed calculation method (d = 4mm, air-gap between beams)

The measured test setup consisted of the rectangular copper conductor ("20x4") formed in U-shape, and supporting clamps ("50x10"). Since the distance between two arms of the conductor was quite small (d=4mm), and comparable to its thickness, one could expect the strong non-linear behaviour. In fact, the measurements managed by laser sensors placed in the middle of beam's height confirmed it. The recorded value of beam's deformation was on the level of 2.6mm (for the current equal to 2.4kA), while the result provided by the simplified analytical theory gave about 3.2mm. The numerical procedure, as described by this paper, showed the beam's deformation on the level of 2.51mm, Figure 6, which is close to the measured data (below 5% of the difference).

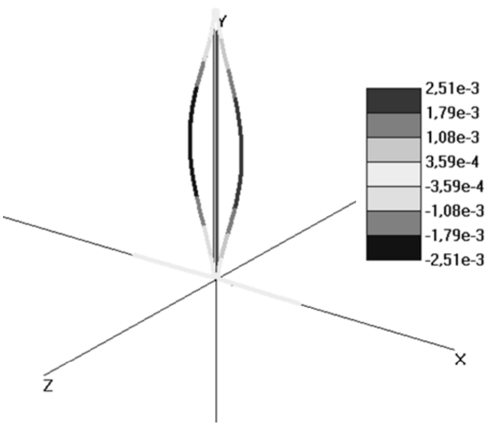

Fig.6. The calculated displacement Ux [m], of the circuit under study. Scale exaggerated. 150 Finite Elements used

Conclusions

The numerical procedure for fast calculations of the busbar structures has been shown in this paper. The presented algorithm utilizes the classical theory described by Biot-Savart and Laplace' laws, and introduces them into FEM formulation of general-purpose 1D beam element. Thanks to this approach, the electro-magnetic, as well as mechanical response of analysed busbar structures can be calculated as fast as analytical equations, but with the flexibility in modelling of FEM software packages. Since modern spreadsheet programs can cope with matrix operations, the proposed algorithm was coded within an ordinary MS/Excel file, what drastically simplifies the usage. The verification and validation process managed for simple and complex busbar geometries, as well as for linear and non-linear cases confirmed high quality of the provided results (below 5% of error), what allows for productive engineering applications. The system can be equally applied in designing of busbars for LV systems and MV switchgears subjected to nominal and short-circuit forces; in analysis of mechanical withstand for HV substation equipment, but also for studying the forces acting on the transformer windings.

REFERENCES

[1] Schaffer G., Electrodynamic forces appearing in electric substations on a short-circuit, *Review Brown Boveri*, (1970), nr 162, 22-31

[2] Labridis D.P., Dokopoulos P.S., Electrodynamic Forces in Three-Phase Busbars with Rectangular Cross-Sections, *IEEE Trans. Power Delivery*, Vol. 11, (1996), nr 2, 793-800

[3] ABB Switchgear Manual, 11th edition, (2006)

[4] IEC 60865-1: Short-circuit currents – calculation of effects

[5] IEC 60909-0: Short-circuit currents in three-phase a.c. systems

[6] IEC TC 73/ CIGRE SC 23 WG11: The mechanical effects of short-circuit currents in open air substations, Vol. 105, (1996)

[7] Legrand, Busbars and distributions - Power Guide, (2009)

[8] Thierry J-P., Kilindjian Ch., Electrodynamic Forces on Busbars in LV Systems, *Cahier Technique Merlin Gerin*, (1996) nr 162

[9] Sigerlind L.J., Applied Finite Element Analysis, John Wiley and sons, (1994)

[10] Bathe K.J., Finite Element Procedures, Prantice Hall, (1996)

[11] Zienkiewicz O.Z., The Finite Element Method, Vol.1 – Basis, B & H, (2000)

[12] Hutton D.V., Fundamentals of Finite Element Analysis, McGraw-Hill, (2004)

[13] Dassault Systèmes Simulia Corp., ABAQUS 6.12, Theory Manual, (2012)

[14] ANSYS, Inc., Ansys Release 12, Theory Reference, (2012)

***Authors**: dr inż. Tomasz Nowak, ABB, Corporate Research Center, ul. Starowiślna 13a, 30-139 Kraków, E-mail: Tomasz.Nowak@pl.abb.com; dr inż. Krzysztof Dudek, ABB, Corporate Research Center, ul. Starowiślna 13a, 30-139 Kraków, E-mail: Krzysztof.Dudek@pl.abb.com; mgr. inż. Piotr Piekarski, ABB, Medium Voltage Products, ul. Leszno 59, 06-300 Przasnysz, E-mail Piotr.Piekarski@pl.abb.com.*

The correspondence address is:
e-mail: tomasz.nowak@pl.abb.com